

## Electrostatic depletion forces between planar surfaces

M. M. Hatlo, R. A. Curtis, and L. Lue

Citation: *J. Chem. Phys.* **128**, 164717 (2008); doi: 10.1063/1.2908738

View online: <http://dx.doi.org/10.1063/1.2908738>

View Table of Contents: <http://jcp.aip.org/resource/1/JCPSA6/v128/i16>

Published by the [American Institute of Physics](#).

---

### Additional information on *J. Chem. Phys.*

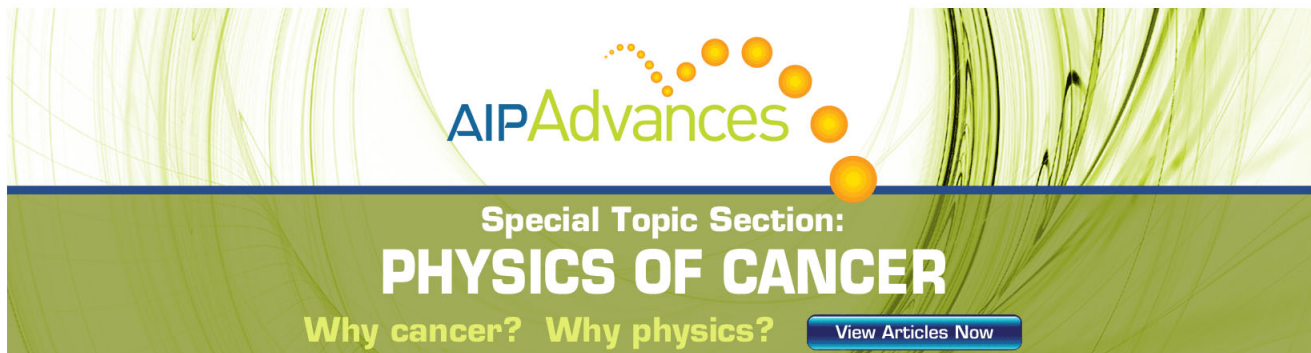
Journal Homepage: <http://jcp.aip.org/>

Journal Information: [http://jcp.aip.org/about/about\\_the\\_journal](http://jcp.aip.org/about/about_the_journal)

Top downloads: [http://jcp.aip.org/features/most\\_downloaded](http://jcp.aip.org/features/most_downloaded)

Information for Authors: <http://jcp.aip.org/authors>

## ADVERTISEMENT



**AIP Advances**

Special Topic Section:  
**PHYSICS OF CANCER**

Why cancer? Why physics? [View Articles Now](#)

## Electrostatic depletion forces between planar surfaces

M. M. Hatlo,<sup>a)</sup> R. A. Curtis, and L. Lue<sup>b)</sup>*School of Chemical Engineering and Analytical Science, The University of Manchester, P.O. Box 88, Sackville Street, Manchester M60 1QD, United Kingdom*

(Received 9 January 2007; accepted 17 March 2008; published online 29 April 2008)

The interaction between two dielectric plates immersed in an electrolyte solution is examined by using a variational perturbation approximation for the grand partition function. This approach differs from previous treatments in that the screening length between the plates is treated as a variational parameter. A key finding is that adjacent to each plate is a layer of ion depletion with thickness given by about one-half of a Bjerrum length. Consequently, for plate-plate separations less than the Bjerrum length, nearly all the electrolyte is excluded from between the plates, and the interaction is given by the sum of a van der Waals interaction and an attractive osmotic depletion force. In contrast to the predictions of previous theories, the interaction between the plates at short range increases with increasing electrolyte concentration and may provide an important contribution to the salt-induced attraction, commonly referred to as salting out. Because the range of the osmotic depletion force is roughly equal to the Bjerrum length, it increases with the square of the valency of the electrolyte. At larger plate-plate separations, the van der Waals interaction is screened as electrolyte enters the space between the plates, leading to an exponential decay of the interactions, as has been previously observed. However, this interaction is slightly stronger than that previously predicted, due to ion depletion from the surface of the interface, also this effect increases with increasing electrolyte concentration. © 2008 American Institute of Physics.

[DOI: [10.1063/1.2908738](https://doi.org/10.1063/1.2908738)]

### I. INTRODUCTION

Understanding the interactions between macromolecular structures in aqueous electrolyte solutions is of great importance in biology and colloid science, with applications to, among others, membrane biology, protein interactions, electrochemistry, and polymers. Our current intuition about these systems is mainly based on the traditional Poisson–Boltzmann equation combined with a van der Waals interaction [Derjaguin–Landau–Verwey–Overbeek (DLVO) theory]. However, DLVO theory suffers from many inadequacies, and improvements have incorporated effects of ion size and ion-dependent dispersion interactions,<sup>1</sup> ion-ion correlations,<sup>2,3</sup> variations in surface charge density, and the effect of salt on the zero-frequency van der Waals interaction.<sup>4–6</sup> In many instances, DLVO theory either overpredicts the repulsion (or underestimates the attraction) between surfaces. A good example is given by the observed electrostatic attraction between similarly charged surfaces in solutions containing divalent ions, an effect which has been rationalized by considering correlations in ion distributions.<sup>2,3,7</sup> However, other questions remain unsolved such as determining the molecular origin of the salt-enhanced attraction between surfaces in moderately concentrated electrolyte solutions,<sup>8</sup> often referred to as salting out.

One possible mechanism for electrostatic enhanced attraction between surfaces is due to depletion forces. This idea can be traced back to Asakura and Osawa,<sup>9</sup> who showed

that an effective attraction between colloids is induced by the addition of polymers to the solution. The attraction arises from the depletion of the polymers from between the colloids due to excluded volume forces. The effect of excluded volume forces on ion distributions about surfaces leads to a depletion layer due to the finite ion size.<sup>10</sup> More significant ion depletion can occur for other reasons, such as repulsive image forces which arise between ions and low dielectric boundaries. Wagner<sup>11</sup> and Onsager and Samaras<sup>12</sup> demonstrated that the image-force induced exclusion of ions from an air-water interface was the molecular origin for the positive surface tension increment of salt solutions. In the absence of a dielectric boundary (i.e., where the surfaces have the same dielectric constant as the solution), ions will be excluded from around surfaces due to a solvation effect where the ions prefer to be in a fully screened environment far from the surface.<sup>13,14</sup> The effects of ion depletion on surface-surface interactions have been shown to lead to enhanced attraction in some cases.<sup>10,15</sup> More specifically, within the primitive model, image forces enhance the effects of ion-ion correlations and can lead to either enhanced attraction or repulsion over the predictions of mean field theories.<sup>16–19</sup>

In this work, we attempt to elucidate the salt-induced interactions between colloidal particles by examining the interaction between two, uncharged semi-infinite dielectric plates. These plates are immersed in an electrolyte solution of point ions with charge  $\pm q$  contained in a continuum solvent of dielectric constant  $\epsilon$ . The confined solution is in equilibrium with a bulk reservoir. The force between the plates is determined by using a variational field theoretic approach

<sup>a)</sup>Electronic mail: [maris.hatlo@postgrad.manchester.ac.uk](mailto:maris.hatlo@postgrad.manchester.ac.uk).<sup>b)</sup>Electronic mail: [leo.lue@manchester.ac.uk](mailto:leo.lue@manchester.ac.uk).

which has been previously used to study electrolytes near planar and spherical dielectric interfaces as well as the forces between these interfaces.<sup>6,13</sup> Ion-ion correlation effects, image forces, and the zero-frequency van der Waals interaction by the ions<sup>4</sup> are all self-consistently included in the model. Here, the theory differs from previous field theoretic approaches,<sup>6,13</sup> in that the screening effectiveness of the confined electrolyte solution is taken as a variational parameter and, consequently, is not the same as that in the bulk reservoir and varies with plate separation. A significant result is that an ion-depletion layer with thickness of about one-half to one Bjerrum length is adjacent to each plate. The reduced electrolyte concentration between the plates leads to a short-ranged force with a range of one Bjerrum length and with a magnitude proportional to the osmotic pressure of the bulk solution.

The paper is organized as follows. In Sec. II, the basic theory behind the variational approach is reviewed. In Sec. III, this theory is applied to study the properties of electrolytes next to a single dielectric interface. The mechanisms for the formation of the electrolyte depletion layer are examined, as well as the dependence of its properties on the electrolyte concentration, and the dielectric constant of the interface and its influence on the surface tension. In Sec. IV, we examine the forces between two dielectric plates that are immersed in an electrolyte solution. In this case, the properties of the depletion layers depend on the spacing between the plates. These properties, in turn, affect the forces between the plates. The implications of this study on the salting-out effect are discussed. Finally, the main findings of this work are summarized in Sec. V.

## II. THEORY

In this work, we consider a system of ions immersed in a continuum solvent with dielectric constant  $\epsilon$ . The absolute temperature of the system is  $T$ , and the chemical potential of ion species  $\alpha$  is  $\gamma_\alpha$  (in units of  $k_B T$ , where  $k_B$  is the Boltzmann constant). In addition, there is a spatially varying dielectric  $\epsilon(\mathbf{r})$  through the system due to the possible presence of dielectric bodies. This inhomogeneous dielectric constant gives rise to zero-frequency dispersion interactions between the dielectric bodies.<sup>4,6</sup> By the use of the Hubbard–Stratonovich transformation,<sup>20,21</sup> the grand partition function  $Z_G$  for this system can be expressed as a functional integral,<sup>14,22–24</sup>

$$Z_G[\gamma] = \frac{1}{\mathcal{N}_0} \int \mathcal{D}\psi(\cdot) \times \exp \left\{ -\frac{1}{2\beta} \int d\mathbf{r} d\mathbf{r}' \psi(\mathbf{r}) G_0^{-1}(\mathbf{r}, \mathbf{r}') \psi(\mathbf{r}') + \ln Z_G^{\text{ref}}[\gamma - q_i \psi + \beta e^{\text{se}}] + \ln \frac{\mathcal{N}_0}{\mathcal{N}_{\text{free}}} \right\}, \quad (1)$$

where  $\beta = (k_B T)^{-1}$ ,  $Z_G^{\text{ref}}$  is the grand partition function of the reference system (i.e., the system without electrostatic interactions),  $G_0$  is the Green's function of the electrostatics problem,<sup>25</sup>

$$-\frac{1}{4\pi} \nabla \cdot \epsilon(\mathbf{r}) \nabla G_0(\mathbf{r}, \mathbf{r}') = \delta^3(\mathbf{r} - \mathbf{r}'), \quad (2)$$

$G_{\text{free}}$  is the Green's function in the absence of spatial variations of the dielectric constant (i.e.,  $\epsilon$  is a constant),

$$G_{\text{free}}(\mathbf{r}, \mathbf{r}') = \frac{1}{\epsilon |\mathbf{r} - \mathbf{r}'|}, \quad (3)$$

and

$$\mathcal{N}_{\text{free}} = \int \mathcal{D}\psi(\cdot) \times \exp \left[ -\frac{1}{2\beta} \int d\mathbf{r} d\mathbf{r}' \psi(\mathbf{r}) G_{\text{free}}^{-1}(\mathbf{r}, \mathbf{r}') \psi(\mathbf{r}') \right].$$

The quantity  $e_\alpha^{\text{se}}$  represents the self-energy of an ion, which is the direct interaction of the ion with the field generated by its own charge, and is given by

$$e_\alpha^{\text{se}} = \frac{q_\alpha^2}{2} G_{\text{free}}(\mathbf{r}, \mathbf{r}).$$

The term  $\ln \mathcal{N}_0 / \mathcal{N}_{\text{free}}$  represents the zero-frequency dispersion interaction caused by an inhomogeneous dielectric.<sup>4,6</sup>

The expression for  $Z_G$  given in Eq. (1) is formally exact. Physically, it states that the grand partition function of a system with electrostatic interactions is equal to the grand partition function of a system without electrostatic interactions in the presence of a fluctuating external field. This external field varies according to a Gaussian distribution, with a spatial correlation given by  $\beta G_0(\mathbf{r}, \mathbf{r}')$ . Unfortunately, it is not possible to analytically evaluate the functional integral for any except the simplest systems. However, a number of different approximation methods can be used. One such method is the loop expansion, which has recently been applied to several problems involving electrolyte solutions at interfaces.<sup>6,26,27</sup>

In the present work, the partition function is approximated by using the variational method,<sup>28,29</sup> an approach which has previously been successfully applied to a wide variety of electrolyte problems.<sup>14,24,30,31</sup> In this method, averages are taken with respect to the Gaussian Hamiltonian,

$$H_{\mathcal{K}}[\psi] = -\frac{1}{2\beta} \int d\mathbf{r} d\mathbf{r}' [i\psi(\mathbf{r}) - i\bar{\psi}(\mathbf{r})] G_{\mathcal{K}}^{-1}(\mathbf{r}, \mathbf{r}') \times [i\psi(\mathbf{r}') - i\bar{\psi}(\mathbf{r}')].$$

The function  $i\bar{\psi}(\mathbf{r})$  represents the mean value of the electric potential in the system. The Green's function  $G_{\mathcal{K}}$  controls the strength of the fluctuations of the electric potential and is given by

$$G_{\mathcal{K}}^{-1}(\mathbf{r}, \mathbf{r}') = G_0^{-1}(\mathbf{r}, \mathbf{r}') + \mathcal{K}(\mathbf{r}, \mathbf{r}'),$$

where  $\mathcal{K}$  is a nonlocal screening function, which is due to the presence of mobile charged particles. It is convenient to split the Green's function of the system into a bulk part and a term representing the influence of any dielectric bodies,

$$G_{\mathcal{K}}(\mathbf{r}, \mathbf{r}') = G_{\mathcal{K}}^{\text{bulk}}(\mathbf{r}, \mathbf{r}') + \delta G_{\mathcal{K}}(\mathbf{r}, \mathbf{r}'), \quad (4)$$

where the second term is directly related to the potential of mean force between the ions and the dielectric bodies. Within the first order variational approximation, the grand partition function is

$$\begin{aligned} \ln Z_G[\gamma] \geq & \frac{1}{2\beta} \int d\mathbf{r} d\mathbf{r}' i\bar{\psi}(\mathbf{r}) G_0^{-1}(\mathbf{r}, \mathbf{r}') i\bar{\psi}(\mathbf{r}') \\ & - \frac{1}{2} \int_0^1 d\xi \text{Tr} \mathcal{K}(G_{\xi\mathcal{K}} - G_{\mathcal{K}}) + \ln \frac{\mathcal{N}_0}{\mathcal{N}_{\text{free}}} \\ & + \langle \ln Z_G^{\text{ref}}[\gamma - qi\psi - qi\bar{\psi} + \beta e^{\text{se}}] \rangle_{\mathcal{K}}, \end{aligned} \quad (5)$$

where the averages  $\langle \dots \rangle_{\mathcal{K}}$  are defined as

$$\langle (\dots) \rangle_{\mathcal{K}} = \frac{1}{\mathcal{N}_{\mathcal{K}}} \int \mathcal{D}\psi(\cdot) (\dots) e^{-H_{\mathcal{K}}[\psi]},$$

$$\mathcal{N}_{\mathcal{K}} = \int \mathcal{D}\psi(\cdot) e^{-H_{\mathcal{K}}[\psi]},$$

and

$$\mathcal{N}_0 = \int \mathcal{D}\psi(\cdot) \exp \left[ -\frac{1}{2\beta} \int d\mathbf{r} d\mathbf{r}' \psi(\mathbf{r}) G_0^{-1}(\mathbf{r}, \mathbf{r}') \psi(\mathbf{r}') \right].$$

This approximation provides a rigorous lower bound to the grand partition function so that the exact value of the grand partition function must be greater than the approximate value calculated by using Eq. (5).

The approximated partition function depends on the form of the arbitrary functions  $\bar{\psi}$  and  $\mathcal{K}$ , whereas the exact grand partition function must be independent of these choices. The idea of the variational method is to make some approximation to the grand partition function and to choose the functions  $\bar{\psi}$  and  $\mathcal{K}$  such that the conditions

$$\frac{\delta}{\delta i\bar{\psi}(\mathbf{r})} \ln Z_G[\gamma] = 0, \quad (6)$$

$$\frac{\delta}{\delta \mathcal{K}(\mathbf{r}, \mathbf{r}')} \ln Z_G[\gamma] = 0, \quad (7)$$

are satisfied.

For a system of point charges, the only forces between the ions are due to electrostatic interactions. In the absence of these interactions, the system behaves as an ideal gas. Therefore, the partition function of the reference system is

$$Z_G^{\text{ref}}[\gamma] = \sum_{\alpha} \Lambda_{\alpha}^d \int d\mathbf{r} e^{\gamma_{\alpha}(\mathbf{r})}, \quad (8)$$

where  $\Lambda_{\alpha}$  is the thermal wavelength and  $\gamma_{\alpha}$  is the chemical potential of an ion of type  $\alpha$ . The density of the ions in the system is given by the relation

$$\rho_{\pm}(\mathbf{r}) = \frac{\delta \ln Z_G[\gamma]}{\delta \gamma_{\pm}(\mathbf{r})}. \quad (9)$$

Applying Eq. (6) to the approximation for  $\ln Z_G$  given in Eq. (5) yields

$$-\frac{1}{4\pi} \nabla [\epsilon(\mathbf{r}) \nabla i\bar{\psi}(\mathbf{r})] = \sum_{\alpha} \beta q_{\alpha} \rho_{\alpha}(\mathbf{r}), \quad (10)$$

which is the Poisson equation. Solving Eq. (7) gives an expression for the screening function,

$$\mathcal{K}(\mathbf{r}, \mathbf{r}') = \delta(\mathbf{r}, \mathbf{r}') \beta \sum_{\alpha} q_{\alpha}^2 \rho_{\alpha}(\mathbf{r}), \quad (11)$$

where the spatially varying density  $\rho_{\alpha}(\mathbf{r})$  of ion species  $\alpha$  is given by

$$\rho_{\alpha}(\mathbf{r}) = \rho_{\alpha}^{\text{bulk}} \exp \left[ -\frac{\beta q_{\alpha}^2}{2} \delta G_{\mathcal{K}}(\mathbf{r}, \mathbf{r}) - q_{\alpha} i\bar{\psi}(\mathbf{r}) \right]. \quad (12)$$

In the general case, this result gives two coupled equations to solve for  $\mathcal{K}(\mathbf{r}, \mathbf{r}')$  and  $i\bar{\psi}(\mathbf{r})$ . The electrostatic potential  $i\bar{\psi}(\mathbf{r})$  will be nonzero if there are preferential ion-surface interactions, as occur for systems with asymmetric electrolytes or ion-specific forces. In the following sections, we restrict the analysis to symmetric electrolytes, in which case Eq. (12) yields  $i\bar{\psi}(\mathbf{r})=0$ .

### III. SINGLE-PLATE GEOMETRY

In this section, we consider a system with a single planar interface separating two regions. The first region contains electrolytes immersed in a solvent of uniform dielectric constant  $\epsilon$ . The second region consists of a dielectric body (of uniform dielectric constant  $\epsilon'$ ) which excludes the electrolytes. The electrolyte solution is in equilibrium with a bulk reservoir, in which the number density of ions of type  $\alpha$  is  $\rho_{\alpha}^{\text{bulk}}$ . This system could represent an interface formed between a salt solution and a solid substrate or a bulk vapor phase.

Using the first order variational theory to calculate the behavior of this system requires knowledge of the Green's function  $G_{\mathcal{K}}$ . However, analytically determining the Green's function that corresponds to the solution of the variational equation [see Eq. (11)] is not generally possible, even for this simple geometry. To overcome this difficulty, a trial form is chosen for the screening function  $\mathcal{K}$  such that the Green's function  $G_{\mathcal{K}}$  can be obtained in analytical form. The parameters that characterize the form of  $\mathcal{K}$  are then adjusted to maximize the value of the grand partition function. Previous works on these systems have chosen a form for  $\mathcal{K}$  that is equal to 0 for positions inside the dielectric body and equal to a constant for the region outside the dielectric body. In the next sections, the predictions of this approximation are compared to those of a more sophisticated model, where a region adjacent to the surface of varying thickness and screening ability is considered.

### A. Uniform screening

The simplest form for the screening function is given by

$$\mathcal{K}(\mathbf{r}, \mathbf{r}') = \delta(\mathbf{r}, \mathbf{r}') \frac{\epsilon}{4\pi} \begin{cases} \kappa^2 & \text{inside electrolyte} \\ 0 & \text{inside dielectric body.} \end{cases} \quad (13)$$

The screening function vanishes inside the dielectric body due to the absence of electrolytes in this region. Outside the dielectric body, the screening is assumed to be uniform, and the strength of the screening is used as a variational parameter to be found by maximizing the grand partition function, i.e.,

$$\frac{\partial \ln Z_G}{\partial \kappa} = 0. \quad (14)$$

The Green's function corresponding to the screening function given by Eq. (13) can be determined analytically and is given by<sup>32</sup>

$$G_{\mathcal{K}}(\mathbf{r}, \mathbf{r}') = \frac{e^{-\kappa|\mathbf{r}-\mathbf{r}'|}}{\epsilon|\mathbf{r}-\mathbf{r}'|} + \delta G_{\mathcal{K}}(\mathbf{r}, \mathbf{r}'), \quad (15)$$

where

$$\delta G_{\mathcal{K}}(\mathbf{r}, \mathbf{r}') = -\frac{2\pi}{\epsilon} \int_{\mathbf{p}} \frac{\Delta(p; \eta, \kappa)}{(p^2 + \kappa^2)^{1/2}} \times e^{-(p^2 + \kappa^2)^{1/2}(z+z')} e^{-ip_x(x-x') - ip_y(y-y')}, \quad (16)$$

where  $z$  is the distance from the dielectric interface, and  $\Delta(p; \eta, \kappa)$  is given by

$$\Delta(p; \eta, \kappa) = \frac{\eta p - (\kappa^2 + p^2)^{1/2}}{\eta p + (\kappa^2 + p^2)^{1/2}}, \quad (17)$$

in which  $\eta = \epsilon' / \epsilon$  is the dielectric constant ratio.

The first term of Eq. (15) is the Green's function for a bulk electrolyte, while the second term on the left side accounts for the influence of the dielectric interface. The quantity  $\delta G_{\mathcal{K}}(\mathbf{r}, \mathbf{r}')$  is equal to the potential of mean force between an ion of unit charge located at position  $\mathbf{r}$  and the dielectric interface,

$$\begin{aligned} \delta G_{\mathcal{K}}(\mathbf{r}, \mathbf{r}) &= -\frac{1}{\epsilon} \int_0^\infty dp \frac{p \Delta(p; \eta, \kappa)}{(p^2 + \kappa^2)^{1/2}} e^{-2(p^2 + \kappa^2)^{1/2} z} \\ &= -\left( \frac{\eta - 1}{\eta + 1} \right) \frac{e^{-2\kappa z}}{2\epsilon z} \\ &\quad - \frac{2\eta}{\eta + 1} \frac{\kappa}{\epsilon} \int_1^\infty dx \frac{\sqrt{x^2 - 1} - x}{\eta \sqrt{x^2 - 1} + x} e^{-2x\kappa z}. \end{aligned} \quad (18)$$

The first term on the right side of Eq. (18) gives the screened interaction energy between a charge and its own image. This term is attractive when  $\eta > 1$ , as occurs in the case of an electrolyte-metal interface, or repulsive for  $\eta < 1$ , which is the case for the electrolyte-air interface or electrolyte-colloid interface. The second term results from the exclusion of ions about the dielectric body and always gives a repulsive contribution to the potential of mean force. This repulsion arises from the fact that ions prefer to be surrounded by other ions

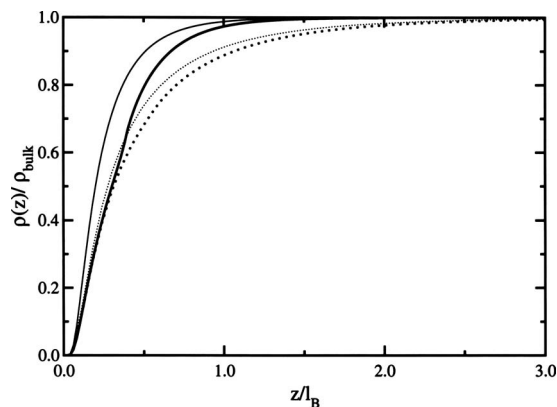


FIG. 1. The density as a function of position for  $\eta=0$  and (i)  $\kappa_{\text{bulk}} l_B=1.5$  (solid line) and (ii)  $\kappa_{\text{bulk}} l_B=0.5$  (dotted line). The thin lines are for  $\kappa_1 = \kappa_{\text{bulk}}$ , and the thick lines give the result when  $\kappa_1$  and  $h$  are optimized.

to screen their own charge and, consequently, lower the energy of the system. The charge of an ion located near the interface is less completely screened relative to that of an ion in the bulk solution due to the presence of the electrolyte-free body. Consequently, ions are repelled from the interface. We refer to this phenomenon as the solvation effect.

Because we are using a point particle model [see Eq. (8)], excluded volume effects are not included, and the theory as such is only valid for low packing fractions. When the packing fraction of the ions becomes significant, ions feel an effective attraction toward the wall, an effect that may dominate the solvation force discussed above. Monte Carlo simulation studies show that excluded volume effects start to dominate the electrostatic solvation effect at concentrations above about  $1.0M$ . Simulations at  $0.1M$  (Ref. 33) and  $0.5M$  (Ref. 34) show ion depletion, while simulations at  $1.0M$  show a slight absorption of the ions,<sup>33</sup> for  $\eta=1.0$  (i.e., no mismatch in the dielectric constants). Thus, the point ion treatment is expected to qualitatively describe the behavior of ions at interfaces for systems with ion concentrations below  $1M$ . What is more interesting is the case when  $\eta \approx 0$ ; there, the ions are found to be depleted even for ion concentrations up to  $2.0M$ ,<sup>34</sup> indicating that the electrostatic interactions are the most important factor determining the density profile of the ions. However, at such high densities, the electrostatic interactions are strongly affected by the hard core, and a simple point ion treatment is expected to be insufficient.

The grand partition function is given by

$$\begin{aligned} \ln Z_G &= V \left[ -\frac{\kappa^3}{24\pi} + \sum_{\alpha} \rho_{\alpha}^{\text{bulk}} \right] + A \frac{\kappa^2 \bar{\Delta}}{32\pi} \\ &\quad + \sum_{\alpha} \rho_{\alpha}^{\text{bulk}} \int dz [e^{-(\beta q_{\alpha}^2/2) \delta G_{\mathcal{K}}(z,z)} - 1] + \ln \frac{\mathcal{N}_0}{\mathcal{N}_{\text{free}}}, \end{aligned}$$

where  $\bar{\Delta} = (\eta - 1)/(\eta + 1)$  and  $A$  is the area of the interface. By applying the variational condition for  $\kappa$  [see Eq. (14)], we find that  $\kappa = \kappa_{\text{bulk}}$ , where  $\kappa_{\text{bulk}}^2 = 4\pi\beta \sum_{\alpha} \rho_{\alpha}^{\text{bulk}} q_{\alpha}^2 / \epsilon$ , as expected.

The corresponding density profiles are shown as thin lines in Fig. 1. Within this approach, the ions are desorbed from the dielectric interface when  $\eta < 1$ . This depletion of

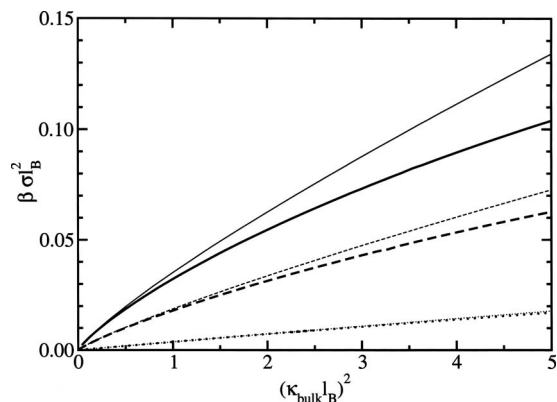


FIG. 2. The surface tension as predicted by the variational theory: (i)  $\eta = 0.0$  (solid line), (ii)  $\eta = 0.5$  (dashed line), and (iii)  $\eta = 1.0$  (dotted line). The thin lines give the result when  $\kappa_1 = \kappa_{\text{bulk}}$ , and the thick lines are from the full variational theory.

ions near the dielectric interface is predominantly driven by repulsive image charge forces but also occurs as a result of the solvation effect. The latter effect is the cause of electrolyte exclusion from an interface separating regions of the same dielectric constant.

The excess surface tension  $\sigma$  is given by the difference between the grand partition function of the confined system and that of a bulk system with the same, temperature, and volume. That is,

$$\beta\sigma = -\frac{1}{A}[\ln Z_G - \ln Z_G^{\text{bulk}}]. \quad (19)$$

The resulting expression for the excess surface tension  $\sigma$  is

$$\beta\sigma = -\frac{\kappa_{\text{bulk}}^2 \bar{\Delta}}{32\pi} - \sum_{\alpha} \rho_{\alpha}^{\text{bulk}} \int_0^{\infty} dz [e^{-(\beta q_{\alpha}^2/2)\delta G_{\mathcal{K}}(z,z)} - 1] - \ln \frac{\mathcal{N}_0}{\mathcal{N}_{\text{free}}}. \quad (20)$$

This expression was previously obtained by Curtis and Lue<sup>14</sup> and is similar to the expression obtained by Wagner<sup>11</sup> and by Onsager and Samaras.<sup>12</sup> The first term on the right side of Eq. (20) is due to electrostatic fluctuation effects, whereas the second term is linked to the interfacial electrolyte density profile, in which depletion of ions gives a positive contribution to the surface tension. We are primarily interested in the change in surface tension due to the addition of ions, which implies that the last term can be neglected as it contributes only to the surface tension of the pure water-air interface. The predictions of Eq. (20) for the excess surface tension are plotted as thin lines in Fig. 2. The surface tension increases with decreasing values of  $\eta$  due to the enhancement of repulsive image forces leading to greater electrolyte depletion.

## B. Incorporation of a depletion layer

The results of the previous section indicate that for  $\eta < 1$ , there is a depletion of ions near an interface due to a combination of image forces and the solvation effect. However, because of the simplistic choice of the form of the screening function [see Eq. (13)], this variation of ion den-

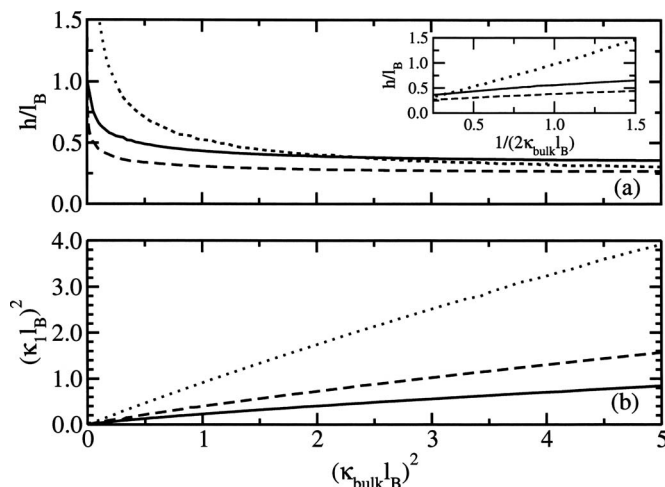


FIG. 3. The variation of the (a) thickness  $h$  and (b) inverse screening length  $\kappa_1$  of the depletion layer with the reduced electrolyte concentration  $(\kappa_{\text{bulk}} l_B)^2$  for (i)  $\eta = 0$  (solid line), (ii)  $\eta = 0.5$  (dashed line), and (iii)  $\eta = 1$  (dotted line). The inset is for the case where  $\eta = 1.0$ .

sity near the interface is not reflected by the screening parameter, which is a constant in this region. By allowing the screening parameter to vary, a better approximation to the partition function can be obtained. In the following approach, we use a screening function of the form

$$\mathcal{K}(\mathbf{r}, \mathbf{r}') = \delta(\mathbf{r}, \mathbf{r}') \frac{\epsilon}{4\pi} \begin{cases} 0, & \text{inside dielectric body} \\ \kappa_1^2, & 0 < z < h \\ \kappa_2^2, & h < z, \end{cases} \quad (21)$$

where  $h$  is the thickness of the depletion layer,  $\kappa_1$  is the inverse screening length inside the depletion layer, and  $\kappa_2$  is the inverse screening length outside the depletion layer. As before, the variational parameters (i.e.,  $h$ ,  $\kappa_1$ , and  $\kappa_2$ ) are obtained by maximizing the grand partition function. Dean and Horgan<sup>13</sup> have used a similar approach in which  $\kappa_1$  is set to 0 over a region next to a planar interface, the thickness of which is chosen to reflect the finite ion size. This approach differs from the one given here in that the values of  $h$  and  $\kappa_1$  are treated as variational parameters and, consequently, the parameters will reflect the ion exclusion which is predominantly driven by image forces. In this case, the width  $h$  of the depletion layer is mainly dependent on the Bjerrum length  $l_B = \beta q_{\alpha}^2 / \epsilon$ , which represents the distance at which two free (in absence of other ions) ions interact with an energy equal to  $k_B T$ . Further, the differences between these approaches will be enhanced for systems with multivalent ions, in which case, the values of  $l_B$  are larger.

For the screening function given by Eq. (21), the corresponding Green's function, for  $0 < z < h$ , is

$$\delta G_{\mathcal{K},1}(z,z) = -\frac{2\pi}{\epsilon} \int_{\mathbf{p}} \times \frac{\Delta_{32} e^{-2K_1(h-z)} + \Delta_{12} e^{-2zK_1} - 2\Delta_{12}\Delta_{32} e^{-2hK_1}}{K_1(1 - \Delta_{12}\Delta_{32} e^{-2hK_1})}, \quad (22)$$

where

$$\Delta_{12} = \frac{\eta p - \sqrt{\kappa_1^2 + p^2}}{\eta p + \sqrt{\kappa_1^2 + p^2}},$$

$$\Delta_{32} = \frac{\sqrt{\kappa_2^2 + p^2} - \sqrt{\kappa_1^2 + p^2}}{\sqrt{\kappa_2^2 + p^2} + \sqrt{\kappa_1^2 + p^2}},$$

and  $K_i = \sqrt{p^2 + \kappa_i^2}$ . For  $z > h$ , the Green's function is given by

$$\delta G_{K,2}(z, z) = -\frac{2\pi}{\epsilon} \int_p e^{-2K_2(z-h)} \frac{\Delta_{32} - \Delta_{12} e^{-2hK_1}}{K_2(1 - \Delta_{12}\Delta_{32}e^{-2hK_1})}. \quad (23)$$

The full expression for the surface tension when including a depletion layer is

$$\begin{aligned} \beta\sigma = & h \frac{\kappa_1^3 - \kappa_2^3}{24\pi} + \frac{\kappa_2^2}{8\pi} \int_0^1 d\zeta \int_0^\infty dp p \left[ \frac{\Delta_{32}(p; \eta, \sqrt{\zeta}\kappa_2, \sqrt{\zeta}\kappa_1)}{(p^2 + \zeta\kappa_2^2)} - \frac{\Delta_{32}(p; \eta, \kappa_1, \kappa_2)}{(p^2 + \kappa_2^2)} \right] - \frac{\kappa_1^2}{8\pi} \int_0^1 d\zeta \int_0^\infty dp p \left[ \frac{\Delta_{32}(p; \eta, \sqrt{\zeta}\kappa_1, \sqrt{\zeta}\kappa_2)}{(p^2 + \zeta\kappa_1^2)} \right. \\ & \left. - \frac{\Delta_{32}(p; \eta, \kappa_1, \kappa_2)}{(p^2 + \kappa_1^2)} \right] - \frac{\kappa_1^2}{32\pi} \frac{\eta - 1}{\eta + 1} + \frac{1}{4\pi} \int_0^\infty dp p \ln[1 - \Delta_{12}\Delta_{32}e^{-2h\sqrt{p^2 + \kappa_1^2}}] \\ & + \frac{\kappa_1^2}{16\pi} \int_0^\infty dp p \frac{e^{-2h\sqrt{p^2 + \kappa_1^2}} (p^2 + \kappa_1^2)^{-1/2} (\Delta_{12} + \Delta_{32})(\Delta_{12}\Delta_{32} - 1) - 4h\Delta_{12}\Delta_{32}}{1 - \Delta_{12}\Delta_{32}e^{-2h\sqrt{p^2 + \kappa_1^2}}} \\ & - \frac{\kappa_2^2}{16\pi} \int_0^\infty dp p \frac{e^{-2h\sqrt{p^2 + \kappa_1^2}} \Delta_{12}(\Delta_{32}^2 - 1)}{(p^2 + \kappa_2^2)(1 - \Delta_{12}\Delta_{32}e^{-2h\sqrt{p^2 + \kappa_1^2}}} - \frac{\kappa_{\text{bulk}}^2}{4\pi} \left\{ \int_0^h dz [e^{(\beta q_d^2/2)(\kappa_1 - \kappa_{\text{bulk}}) - (\beta q_d^2/2)\delta G_{K,1}} - 1] \right. \\ & \left. + \int_h^\infty dz [e^{(\beta q_d^2/2)(\kappa_2 - \kappa_{\text{bulk}}) - (\beta q_d^2/2)\delta G_{K,2}} - 1] \right\}. \quad (24) \end{aligned}$$

The first term in Eq. (24) represents the change in the bulk electrostatic term due to the variation in ion density, while the next four terms give the fluctuation contribution to the free energy of formation of the interface. The next two terms originate from the change in self-energy of the ions due to the presence of the interface. The final term gives the entropic contribution due to changes in ion density near the interface.

As mentioned earlier, the values of the parameters  $h$ ,  $\kappa_1$ , and  $\kappa_2$  need to be determined to evaluate the thermodynamic properties. The value of the inverse screening length  $\kappa_2$  outside the depletion layer is set to that of the bulk electrolyte (i.e.,  $\kappa_2 = \kappa_{\text{bulk}}$ ) as found in Sec. III A. The values of  $\kappa_1$  and  $h$  are numerically found by maximizing the grand partition function. In Fig. 3, the variation of the size of the depletion layer and the screening within the depletion layer with electrolyte concentration is presented. For dilute electrolyte solutions, the thickness of the depletion layer  $h$  rapidly decreases with increasing electrolyte concentration up to a concentration corresponding to  $\kappa_{\text{bulk}}l_B = 1$ . For moderately concentrated electrolyte solutions,  $h$  remains relatively constant and approximately equal to  $0.3l_B$ . Thus, we find a cross-over region near  $\kappa_{\text{bulk}} = l_B$ , below which the depletion layer is linked to the bulk screening length, and above which,  $h$  is independent of electrolyte concentration and is relatively insensitive to the value of  $\eta$ .

In contrast, as shown in Fig. 3(b), the value of  $\kappa_1$  decreases with decreasing values of  $\eta$ , indicating a concomitant decrease in the screening effectiveness. This effect is linked

to the larger electrolyte exclusion arising from the enhanced repulsive image forces. For the case where  $\eta = 0$ , the screening effectiveness next to the surface is about 0.2 times the corresponding bulk value, whereas for the case where  $\eta = 1$ ,  $\kappa_1$  is only slightly less than  $\kappa_{\text{bulk}}$ .

In the case where there is no dielectric interface (i.e.,  $\eta = 1$ ), the size of the depletion layer is only dependent on the bulk screening length and is well approximated by  $h \approx (2\kappa_{\text{bulk}})^{-1}$ , as can be seen from the inset of Fig. 3(a). In this case, depletion is mainly driven by the solvation effect and, therefore, one might expect that the width of the depletion layer is of the size of the screening length.

In Fig. 1, the ion density profile is plotted as thick lines for different values of the bulk concentration. We see that the inclusion of the depletion layer induces more depletion of the electrolyte in the vicinity of the plate. This enhanced exclusion is induced by the extended range of the image charge and solvation forces caused by a discontinuity in the screening ability.

By including the depletion layer with an associated reduced screening, several additional terms appear in the expression for the surface tension. These extra terms are due to electrostatic fluctuation effects associated with the depletion layer. Figure 2 shows the surface tension as predicted by Eq. (24). The result of the full variational theory gives a lower surface tension as compared to Eq. (20). This extra negative contribution can be mainly attributed to the first term in Eq. (24), which gives the difference in bulk electrostatic energy evaluated at the bulk ion density and that at the electrolyte

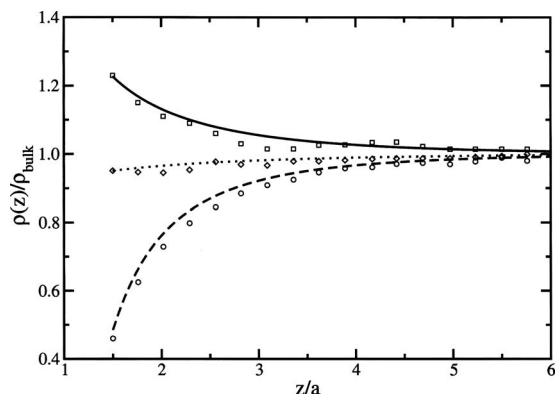


FIG. 4. Comparison between this work (lines) and simulation data by Henderson *et al.* (Ref. 34) (symbols). Note that  $l_B/h=2.32$  and  $\kappa_1=0$ . (i)  $\epsilon_1=\infty$ ,  $\epsilon_2=80$ , and  $\epsilon_3=80$  (solid line and squares), (ii)  $\epsilon_1=80$ ,  $\epsilon_2=80$ , and  $\epsilon_3=80$  (dotted line and circles), and (iii)  $\epsilon_1=\infty$ ,  $\epsilon_2=6$ , and  $\epsilon_3=80$  (dashed line and diamonds).

density near the plates. As a result of the variational principle, the surface tension predicted by this theory gives an upper bound to the actual surface tension of a point charge electrolyte.

### C. Comparison with simulation

To quantitatively validate the theory developed in this section, we compare predictions with recent Monte Carlo simulations by Henderson *et al.*<sup>34</sup> of an electric double layer near an uncharged electrode. In this simulation, the ions are modeled as charged hard spheres confined to a region  $z > \delta$  with constant dielectric coefficient  $\epsilon_3$ . For  $0 < z < \delta$ , there is an ion free layer of dielectric constant  $\epsilon_2$ ; this layer is commonly known as a Helmholtz or Stern layer and accounts for exclusion of ions from the surface due to effects not directly included in the theory, normally related to the solvent or specific properties of the surface. The electrode is located in the region  $z < 0$  and has a dielectric constant  $\epsilon_1$ . The size of the depletion layer (Stern layer) is for simplicity taken to be the same as the ion diameter  $a$  (i.e.,  $\delta=a$ ); consequently, the distance of closest approach of an ion center to the electrode is  $3a/2$ . The theory developed in the previous sections can be extended to include a third dielectric layer that is inaccessible to electrolytes. The only change in the theory is to let

$$\Delta_{32} = \frac{\sqrt{\kappa_2^2 + p^2} - \eta' p}{\sqrt{\kappa_2^2 + p^2} + \eta' p},$$

where  $\eta' = \epsilon_2/\epsilon_3$ . Since the ions are excluded from the depletion region,  $\kappa_1=0$ .

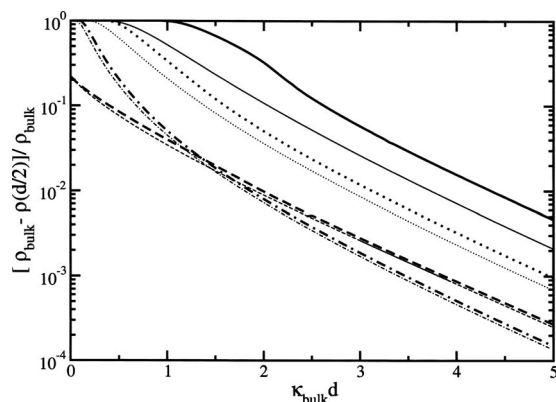


FIG. 5. The density in the middle of the plates as a function of plate separation for (i)  $\kappa_{\text{bulk}}l_B=1.5$ ,  $\eta=0$  (solid line), (ii)  $\kappa_{\text{bulk}}l_B=0.5$ ,  $\eta=0$  (dotted line), (iii)  $\kappa_{\text{bulk}}l_B=0.5$ ,  $\eta=1$  (dashed line), and (iv)  $\kappa_{\text{bulk}}l_B=0.1$ ,  $\eta=0$  (dashed-dotted line). The thin lines are for  $\kappa_1=\kappa_{\text{bulk}}$ , and the thick lines give the result when  $\kappa_1$  and  $h$  are optimized.

In Fig. 4, the ion density profiles predicted by this work are compared to the simulation results of Henderson *et al.*,<sup>34</sup> for a bulk electrolyte concentration of  $\rho_{\text{bulk}}=0.05M$ ; corresponding to a bulk screening  $\kappa_{\text{bulk}}l_B=0.52$ . The theoretical results are in good agreement with the Monte Carlo simulations. Better agreement could be obtained if a more sophisticated form for the screening function was used.

## IV. TWO-PLATE GEOMETRY

In this section, we examine an electrolyte solution of dielectric constant  $\epsilon$  that is confined between two semi-infinite plates separated by a distance  $d$  from each other. As before, the plates have a dielectric constant  $\epsilon'$  and occupy a region which is inaccessible to electrolytes. The confined electrolyte solution is considered to be in equilibrium with a bulk electrolyte solution at ion concentration  $\rho_{\alpha}^{\text{bulk}}$ .

To account for regions of ion exclusion near the interfaces, we use a screening function of the form

$$\mathcal{K}(\mathbf{r}, \mathbf{r}') = \delta(\mathbf{r}, \mathbf{r}') \frac{\epsilon}{4\pi} \begin{cases} 0, & \text{inside dielectric body} \\ \kappa_1^2, & 0 < z < h \\ \kappa_2^2, & h < z < d-h \\ \kappa_1^2, & d-h < z < d. \end{cases}$$

The difference between the Green's function corresponding to the confined electrolyte and that of the bulk electrolyte,  $\delta G_{\mathcal{K}}$ , is given by

$$\begin{aligned} \delta G_{\mathcal{K}}(z, z) = & -\frac{2\pi}{\epsilon} \int_{\mathbf{p}} \Theta(h-z) \\ & \times \frac{\Delta_{12}\Delta_3 e^{-2K_2 z} + \Delta_4 e^{-2K_2(h-z)} - 2\Delta_4\Delta_{12} e^{-2hK_2}}{\Delta_3 - \Delta_4\Delta_{12} e^{-2hK_2}} \\ & + \Theta(z-h)\Theta(d-h-z) \frac{\Delta_1\Delta_2 e^{-2K_3(z-h)} + \Delta_1\Delta_2 e^{-2K_3(d-h-z)} - 2\Delta_1^2 e^{-2(d-2h)K_3}}{\Delta_2^2 - \Delta_1^2 e^{-2(d-2h)K_3}} \end{aligned}$$



$$+ \Theta(z-d+h) \frac{\Delta_{12}\Delta_3 e^{-2K_2(d-z)} + \Delta_4 e^{-2K_2(z-d+h)} - 2\Delta_4\Delta_{12} e^{-2hK_2}}{\Delta_3 - \Delta_4\Delta_{12} e^{-2hK_2}},$$

where

$$\Delta_1 = \Delta_{12} e^{-2hK_2} - \Delta_{32},$$

$$\Delta_2 = 1 - \Delta_{12}\Delta_{32} e^{-2hK_2},$$

$$\Delta_3 = -\Delta_{32}\Delta_1 e^{-2K_3(d-2h)} - \Delta_2,$$

$$\Delta_4 = -\Delta_1 e^{-2(d-2h)K_3} - \Delta_{32}\Delta_2.$$

Here,  $d$  is the distance between the two plates and  $h$  is the size of the depletion layer. In this work, we set  $\kappa_2 = \kappa_{\text{bulk}}$  and optimize the partition function with respect to the depletion layer screening  $\kappa_1$  and the size of the depletion layer  $h$ . This case, referred to as the full variation treatment, is compared to a less accurate approach in which the screening between the plates is assumed to be uniform (i.e.,  $\kappa_1 = \kappa_{\text{bulk}}$ ).

Within the first order variational approximation, the grand partition function is given by

$$\begin{aligned} \ln Z_G[\gamma] \geq & -V \frac{\kappa_{\text{bulk}}^3}{24\pi} + V \sum_{\alpha} \rho_{\alpha}^{\text{bulk}} - 2Ah \frac{\kappa_1^3 - \kappa_{\text{bulk}}^3}{24\pi} + 2A \sum_{\alpha} \rho_{\alpha}^{\text{bulk}} \int_0^h dz \left( \exp \left[ \frac{\beta q_{\alpha}^2}{2} (\kappa_1 - \kappa_{\text{bulk}}) - \frac{\beta q_{\alpha}^2}{2} \delta G_{\mathcal{K}}(z, z) \right] - 1 \right) \\ & + A \sum_{\alpha} \rho_{\alpha}^{\text{bulk}} \int_h^{d-h} dz \left( \exp \left[ -\frac{\beta q_{\alpha}^2}{2} \delta G_{\mathcal{K}}(z, z) \right] - 1 \right) - \frac{1}{2} \int_0^1 d\xi \text{Tr} \mathcal{K}(\delta G_{\xi\mathcal{K}} - \delta G_{\mathcal{K}}) + \ln \frac{\mathcal{N}_0}{\mathcal{N}_{\text{free}}}. \end{aligned} \quad (25)$$

The first two terms on the right side of Eq. (25) represent the contribution to the grand partition function of an unconfined electrolyte solution. The third term accounts for the shift in the bulk electrostatic contribution due to the reduced screening abilities of the depletion layers. The next two terms are the same as those that appear in the grand partition function for a dielectric plate surrounded by electrolyte solution, as studied in Sec. III A, except that the Green's function corresponds to the confined electrolyte. The last two terms are due to fluctuation effects, where the first term arises from ion correlations, and the last term is the static van der Waals energy in the absence of electrolyte.

In Fig. 5, the midplane electrolyte density is plotted as a function of plate-plate separation. The thick lines refer to the full variational theory; the thin lines are for the case  $\kappa_1 = \kappa_2 = \kappa_{\text{bulk}}$ . For large plate-plate separations (i.e.,  $\kappa_{\text{bulk}} d \gg 1$ ), the midplane density exponentially approaches the bulk value with a length scale given by  $\kappa_{\text{bulk}}$ . In the full variational theory, the depletion layer is larger, an effect that is due to electrostatic correlation effects; an enhanced repulsion is felt by the ions near the dielectric surface due to the low screening layer. This extra repulsion is the result of the solvation effect where the ions would like to be in an environment where they are maximally screened. For these large separations, the thicknesses of the depletion layers are roughly half a Bjerrum length. The layers overlap at a plate-plate separation of about one Bjerrum length, a result that is relatively insensitive to bulk salt concentration. For plate-plate separations of less than one Bjerrum length, the electrolyte density

approaches 0 when  $\epsilon'/\epsilon=0$ . This effect is predominantly driven by image charge forces, as much less ion exclusion is observed for the case where there is no dielectric boundary, as depicted in Fig. 5 (i.e.,  $\epsilon'/\epsilon=1$ ). In the latter case, ion depletion occurs due only to a solvation effect, in which ions prefer to be in the fully screened bulk environment versus near the impenetrable plates which have no screening ability.

The variation of the thickness and the associated screening length of the depletion layer with plate-plate separation are plotted in Fig. 6. For  $\eta=0$  (thick lines) and plate-plate separations of less than approximately one Bjerrum length, the depletion layer corresponds to the entire solution (i.e.,  $h=d/2$ ) as reflected by a linear relation between  $h$  and  $d$ . Also, over these separations, the depletion layer have little ability to screen charge (i.e.,  $\kappa_1 \approx 0$ ). For plate separations larger than one Bjerrum length, the thickness of the depletion layer exponentially decays toward the value corresponding to a single plate (see Sec. III). Similarly, the screening factor  $\kappa_1$  rapidly increases from 0 to a finite value at  $d \approx l_B$  after which the value exponentially decays toward the single plate value (see Sec. III). In contrast, when image charge forces are absent as given by the case where  $\eta=1$  (thin lines in Fig. 6), the length scale governing the behavior of the depletion layer thickness and the associated screening is the bulk screening length  $\kappa_{\text{bulk}}$ , rather than  $l_B$ . Here, the depletion of ions is due only to the solvation effect, where the ions prefer to be in more highly screened environments. Thus, the effects of repulsive image charge forces are to both increase the thick-

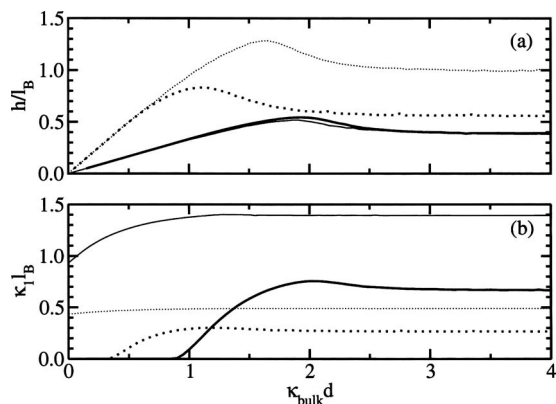


FIG. 6. The variation of the (a) thickness  $h$  and the (b) inverse screening length  $\kappa_1$  of the depletion layer as a function of plate separation  $d$  and (i)  $\kappa_{\text{bulk}} l_B = 1.5$  (solid line) and (ii)  $\kappa_{\text{bulk}} l_B = 0.5$  (dotted line). The thin lines are for  $\eta = 1$ , and the thick lines give the result when  $\eta = 0$ .

ness of the ion-depleted layers (for  $l_B > \kappa_{\text{bulk}}^{-1}$ ) and to reduce the screening effectiveness within these regions.

The net pressure  $p_{\text{int}}$  (force per unit area) acting between the plates is given by the difference between the (osmotic) pressure of the bulk electrolyte  $p_{\text{bulk}}$ , which pushes the plates together, and the (osmotic) pressure  $p$  of the electrolyte between the plates, which pushes the plates apart,

$$\beta p_{\text{int}} = \beta p - \beta p_{\text{bulk}}.$$

The pressure of the electrolyte solution between the plates can be directly obtained from the grand partition function through the relation

$$\beta p = \frac{\partial}{\partial V} \ln Z_G[\gamma]. \quad (26)$$

The force between the two plates, as predicted by the grand partition function given in Eq. (25), is plotted in Fig. 7. The thick lines correspond to the full variational treatment, and the thin lines correspond to setting  $\kappa_1 = \kappa_2 = \kappa_{\text{bulk}}$ . For the latter case, when  $\epsilon' < \epsilon$ , the interaction is dominated by the van der Waals force, which exponentially decays for medium to large plate-plate separations due to screening by the electrolyte according to  $p \propto e^{-2\kappa_{\text{bulk}} d}/d$ . In the absence of a dielec-

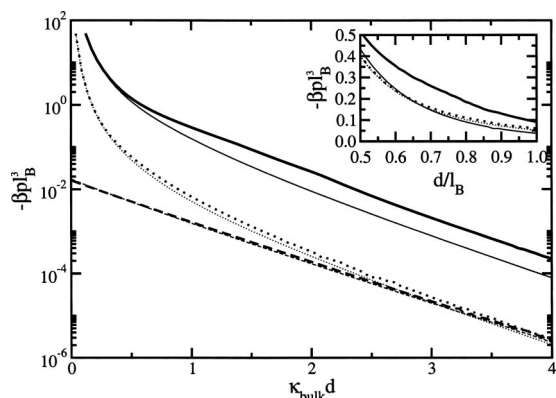


FIG. 7. The pressure as a function of plate separation for: (i)  $\kappa_{\text{bulk}} l_B = 1.5$ ,  $\eta = 0$  (solid line), (ii)  $\kappa_{\text{bulk}} l_B = 0.5$ ,  $\eta = 0$  (dotted line), and (iii)  $\kappa_{\text{bulk}} l_B = 1.5$ ,  $\eta = 1$  (dashed line). The thin lines are for  $\kappa_1 = \kappa_{\text{bulk}}$ , and the thick lines give the result when  $\kappa_1$  and  $h$  are optimized.

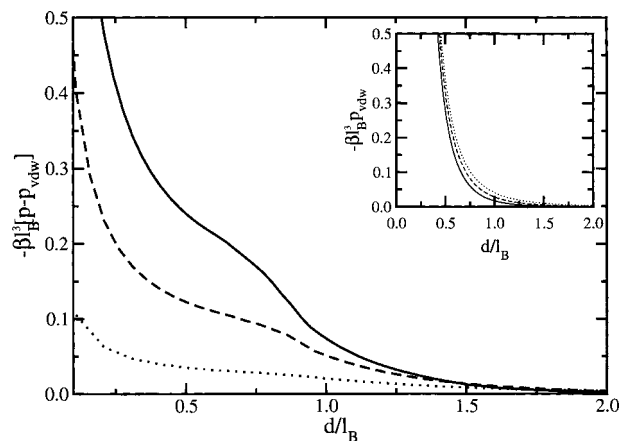


FIG. 8. The difference between the pressure and the screened van der Waals pressure as a function of plate separation for: (i)  $\kappa_{\text{bulk}} l_B = 1.5$  (solid line), (ii)  $\kappa_{\text{bulk}} l_B = 1.0$  (dashed line), and (iii)  $\kappa_{\text{bulk}} l_B = 0.5$  (dotted line). The inset gives the corresponding screened van der Waals pressure.

tric boundary, the van der Waals force is absent; the interaction is due, instead, to electrolyte depletion which causes an imbalance of the osmotic pressure between the plates and in the bulk solution. This interaction also has an exponential decay with distance, although the magnitude of the force is much smaller than that of the van der Waals interaction. The results presented here are similar to the predictions of the loop expansion and other previously developed theories.<sup>6,13,35</sup>

The differences in the predictions of the two treatments are best exemplified when considering the case of  $\eta = 0$  for two regions of plate-plate separation: One region corresponding to separations less than the Bjerrum length and one greater than the Bjerrum length. The former case is depicted in the inset of Fig. 7; in this case, the attraction between the plates is greater when using the variational treatment, an effect that is enhanced with increasing electrolyte concentration. The extra attraction is due to two separate types of effects. Both of these arise from the almost complete exclusion of electrolytes within this region, an effect that has recently been experimentally observed in a study of forces between neutral lipid membranes.<sup>36</sup> For short separations, within the variational treatment, the plates are attracted to each other through a van der Waals interaction<sup>4</sup> that decays as  $1/d^3$  (i.e., it is unaffected by the electrolytes). Superimposed upon the van der Waals force is an attractive, electrolyte depletion force which is enhanced within the variational treatment due to the greater electrolyte exclusion. To clearly show the predictions of the variational theory as compared to the standard screened van der Waals interaction, as derived by Mahanty and Ninham<sup>4</sup> and later by Netz,<sup>6</sup> the difference between the two forces is plotted in Fig. 8. As shown, the difference between the two forces increases with increasing electrolyte concentration, while the standard screened van der Waals interaction has the opposite trend (i.e., the force becomes weaker with increasing bulk electrolyte concentration, see the inset of Fig. 8). The difference between the two treatments becomes comparable or even greater than the standard van der Waals interaction for moderately concentrated solutions ( $\rho_{\text{bulk}} \approx 0.01 - 1.0M$ ,  $\kappa_{\text{bulk}} l_B \approx 0.1 - 2$ ). At

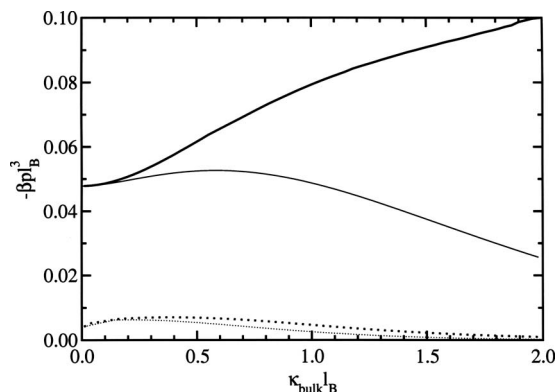


FIG. 9. The variation of the pressure as a function of bulk screening length at constant plate-plate separation for  $\eta=0$ . (i)  $d=l_B$  (solid line) and (ii)  $d=2l_B$  (dotted line). The thin lines are for  $\kappa_1=\kappa_{\text{bulk}}$ , and the thick lines give the result when  $\kappa_1$  and  $h$  are optimized.

separations larger than the Bjerrum length, the intraplate electrolyte concentration increases, and the van der Waals interaction is screened within either treatment, as shown in Fig. 7. However, in the variational approach, the interaction becomes slightly stronger due to the layer of ion depletion about each of the plates.

As mentioned earlier, in the absence of image charge forces, the short-ranged force between the plates is attractive due to the exclusion of ions from between the plates leading to an attractive osmotic depletion force, similar to the one studied by Bratko and Henderson.<sup>18</sup> The exclusion of ions is greater when a low dielectric boundary is present, leading to a much stronger attraction between the plates. For low bulk electrolyte concentrations, the depletion-induced attraction is much smaller than the van der Waals interaction felt at the same distance. However, if the screening length becomes smaller than  $l_B$  (e.g., at high electrolyte concentrations), the osmotic pressure force becomes comparable to the van der Waals interaction, as shown in Fig. 9. Here, the pressure for the case where  $\kappa_1=\kappa_{\text{bulk}}$  is plotted together with the pressure when  $h$  and  $\kappa_1$  is optimized. The difference between the pressures in the two cases can be attributed to the attractive osmotic depletion force and the change in the van der Waals interaction. Since the van der Waals interaction at  $d=l_B$  is almost unaffected by the electrolytes, a good approximation for the magnitude of the osmotic depletion force at this separation is the difference between the total pressure (solid line in Fig. 9) and the van der Waals interaction in the absence of electrolytes [ $-\beta l_B^3 p_{\text{vdW}}^{\kappa_{\text{bulk}}=0}(d=l_B)=0.0477$ ].

At plate separations larger than one Bjerrum length, the electrolyte begins to enter the region between the plates and effectively screens the interaction. This can be seen by considering the case when  $d=2l_B$  in Fig. 9, where the interaction between the plates decreases with increasing electrolyte concentration (dotted line). Note that because we use a point charge model for the electrolytes, the resulting predictions are limited to low packing fractions and  $\kappa_{\text{bulk}} l_B < 4$ , where the mean spacing between the ions is larger than the Bjerrum length.<sup>14</sup>

The results of the variational treatment provide insights into salting-out effects which have been observed for a broad range of solutions containing, for example, micelles,<sup>37</sup> un-

charged polymers,<sup>38</sup> or proteins.<sup>39</sup> In these systems, a salt-induced, short-ranged attraction occurs between the macromolecules in moderate to high ionic strength solutions, where double layer interactions are screened out. In this work, we find that the salt-induced attraction becomes proportional to the osmotic pressure of the salt solution at higher ionic strengths. This result is consistent with recent measurements of the forces between arrays of hydroxypropylcellulose molecules immersed in various aqueous cosolvent systems.<sup>38</sup> In these studies, the measured force is linked to the exponential decay of the confined cosolvent concentration as the interlayer separation decreases; the range of this interaction was found to be independent of the concentration. The characteristic range for this force has previously been associated with the range of hydration forces or with the screening length. We identify this distance as the Bjerrum length, which corresponds to the separation from the dielectric boundary where the interaction energy of an ion with its image charge is equal to  $k_B T$ . The finding that the range is constant with added salt is an important feature of the model; without the variational treatment, the decay length of the depletion interaction would be given by  $\kappa_{\text{bulk}}^{-1}$ , and the interaction would be screened at medium to high ionic strength, as shown in Fig. 9. Further, in the case where there is no dielectric boundary, the exclusion of the confined electrolyte is only a small fraction of the bulk value, in disagreement with the experimental findings. Thus, we expect that image forces play a significant role in determining the forces between surfaces in moderately concentrated electrolyte solutions.

## V. CONCLUSIONS

We have developed a variational theory for electrolyte solutions that explicitly accounts for the ion depletion and reduced screening near dielectric interfaces. This theory was used to examine the force between two uncharged dielectric plates immersed in an electrolyte solution. The force between the plates is composed of a contribution from a van der Waals interaction and from an osmotic depletion force. The van der Waals interaction at short range is nearly unaffected by the electrolyte, as the ion density is very small and, consequently, remains strongly attractive even in moderate to high electrolyte concentrations. The osmotic depletion force is analogous to the depletion forces due to excluded volume, and it becomes proportional to the osmotic pressure of the surrounding bulk solution. This osmotic depletion interaction increases with increasing electrolyte concentration and may contribute to salting-out effects. The force between plates at large separation also increases with increasing electrolyte concentration, a result which is mainly due to ion correlation effects caused by the low screening ability of the depletion layers. At these distances, the force exponentially decays, with a characteristic length scale given by the bulk screening length. Consequently, it rapidly decays in moderately concentrated electrolyte solutions.

Currently, we are working to include excluded volume, induction, and dispersion interactions between the ions themselves, as well as between the ions and the surfaces. The

theory as such would then be applicable to more concentrated electrolyte solutions and would provide insight into ion-specific forces, an understanding of which, has so far remained elusive.

## ACKNOWLEDGMENTS

M.M.H. acknowledges support from an EC Marie Curie Fellowship No. (MEST-CT-2004-503750).

- <sup>1</sup>B. W. Ninham and V. Yaminsky, *Langmuir* **13**, 2097 (1997).
- <sup>2</sup>L. Guldbrand, B. Jönsson, H. Wennerström, and P. Linse, *J. Phys. Chem.* **80**, 2221 (1984).
- <sup>3</sup>J. P. Valleau, R. Ivkov, and G. M. Torrie, *J. Chem. Phys.* **95**, 520 (1991).
- <sup>4</sup>J. Mahanty and B. W. Ninham, *Dispersion Forces* (Academic, London, 1976).
- <sup>5</sup>P. Attard, *J. Phys. Chem.* **93**, 6441 (1989).
- <sup>6</sup>R. R. Netz, *Eur. Phys. J. E* **5**, 189 (2001).
- <sup>7</sup>J. Z. Wu, D. Bratko, H. W. Blanch, and J. M. Prausnitz, *J. Chem. Phys.* **111**, 7084 (1999).
- <sup>8</sup>T. Ghosh, A. Kalra, and S. Garde, *J. Phys. Chem. B* **109**, 642 (2005).
- <sup>9</sup>S. Asakura and F. Oosawa, *J. Chem. Phys.* **22**, 1255 (1954).
- <sup>10</sup>M. N. Tamashiro and P. Pincus, *Phys. Rev. E* **60**, 6549 (1999).
- <sup>11</sup>C. Wagner, *Phys. Z.* **25**, 474 (1924).
- <sup>12</sup>L. Onsager and N. T. Samaras, *J. Chem. Phys.* **2**, 528 (1934).
- <sup>13</sup>D. S. Dean and R. R. Horgan, *Phys. Rev. E* **69**, 061603 (2004).
- <sup>14</sup>R. A. Curtis and L. Lue, *J. Chem. Phys.* **123**, 174702 (2005).
- <sup>15</sup>E. Allahyarov, I. D'Amico, and H. Löwen, *Phys. Rev. Lett.* **81**, 1334 (1998).
- <sup>16</sup>D. Bratko, B. Jönsson, and H. Wennerström, *Chem. Phys. Lett.* **128**, 449 (1986).
- <sup>17</sup>D. Bratko, D. J. Henderson, and L. Blum, *Phys. Rev. A* **44**, 8235 (1991).
- <sup>18</sup>D. Bratko and D. Henderson, *Phys. Rev. E* **49**, 4140 (1994).
- <sup>19</sup>G. M. Torrie, J. P. Valleau, and C. W. Outhwaite, *J. Chem. Phys.* **81**, 6296 (1984).
- <sup>20</sup>R. L. Stratonovich, *Dokl. Akad. Nauk SSSR* **115**, 1097 (1957).
- <sup>21</sup>J. Hubbard, *Phys. Rev. Lett.* **3**, 77 (1959).
- <sup>22</sup>A. L. Kholodenko and A. L. Beyerlein, *Phys. Rev. A* **34**, 3309 (1986).
- <sup>23</sup>L. Lue, N. Zoeller, and D. Blankschtein, *Langmuir* **15**, 3726 (1999).
- <sup>24</sup>L. Lue, *Fluid Phase Equilib.* **241**, 236 (2006).
- <sup>25</sup>J. D. Jackson, *Classical Electrodynamics* (Wiley, New York, 1975).
- <sup>26</sup>A. G. Moreira and R. R. Netz, *Phys. Rev. Lett.* **87**, 078301 (2001).
- <sup>27</sup>G. Tellez, *Phys. Rev. E* **70**, 011508 (2004).
- <sup>28</sup>R. P. Feynman, *Statistical Mechanics: A Set of Lectures* (Addison-Wesley, Redwood, CA, 1972).
- <sup>29</sup>H. Kleinert, *Path Integrals in Quantum Mechanics, Statistics, and Polymer Physics*, 2nd ed. (World Scientific, Singapore, 1995).
- <sup>30</sup>R. R. Netz and H. Orland, *Eur. Phys. J. E* **11**, 310 (2003).
- <sup>31</sup>A. Diehl, M. C. Barbosa, and Y. Levin, *Phys. Rev. E* **56**, 619 (1997).
- <sup>32</sup>R. R. Netz, *Eur. Phys. J. E* **3**, 131 (2000).
- <sup>33</sup>L. B. Bhuiyan, C. W. Outhwaite, D. Henderson, and M. Alawneh, *Mol. Phys.* **105**, 1395 (2007).
- <sup>34</sup>D. Henderson, D. Gillespie, T. Nagy, and D. Boda, *Mol. Phys.* **103**, 2851 (2005).
- <sup>35</sup>P. Attard, D. J. Mitchell, and B. W. Ninham, *J. Chem. Phys.* **89**, 4358 (1988).
- <sup>36</sup>H. I. Petrache, T. Zemb, L. Belloni, and V. A. Parsegian, *Proc. Natl. Acad. Sci. U.S.A.* **103**, 7982 (2006).
- <sup>37</sup>Y. X. Huang, G. M. Thurston, D. Blankschtein, and G. B. Benedek, *J. Chem. Phys.* **92**, 1956 (1990).
- <sup>38</sup>J. Chik, S. Mizrahi, S. Chi, V. A. Parsegian, and D. C. Rau, *J. Phys. Chem. B* **109**, 9111 (2005).
- <sup>39</sup>R. A. Curtis, J. Ulrich, A. Montaser, J. M. Prausnitz, and H. W. Blanch, *Biotechnol. Bioeng.* **79**, 367 (2002).